PFG 2015 / 3, 0231 – 0240
Stuttgart, June 2015

Article

PROSPECT Inversions of Leaf Laboratory Imaging Spectroscopy – a Comparison of Spectral Range and Inversion Technique Influences

Henning Buddenbaum & Joachim Hill, Trier

Keywords: reflectance models, hyperspectral, inversion, LUT, leaf, VNIR, SWIR

Summary: Very high spatial resolution hyperspectral images of leaves were recorded using stationary pushbroom scanners and a translation stage. Separate images were recorded in the visible/near infrared (VNIR, 400 nm – 1000 nm) and in the shortwave infrared range (SWIR, 1000 nm – 2500 nm). We inverted the leaf reflectance model PROSPECT-5b on the image data in two different ways, by numerical inversion and by a lookup table approach. Inversion results using only VNIR images and combined VNIR/SWIR images were compared. We found that the inversion technique has only minor influence on inversion results, but the spectral range of the input data is crucial for some variables: While results for the PROSPECT structure parameter N, chlorophyll content (Cab), carotenoid content (Car) and brown pigments (Cbrown) are similar for both input datasets, results for water content (Cw) and dry matter (Cm) are not correlated between VNIR inversion and VNIR/SWIR inversion. Laboratory-based imaging spectroscopy in combination with radiative transfer model inversion is a technique capable of mapping chemical leaf parameters on a sub-millimetre scale.

Zusammenfassung: *PROSPECT-Inversionen hyperspektraler Laborbilder von Blättern – Ein Vergleich der Einflüsse des Spektralbereichs und der Inversionstechnik*. Höchstaufgelöste hyperspektrale Bilddatensätze von Blättern wurden mit einem stationären Pushbroom-Scanner mit einem Translationsschlitten aufgenommen. Dabei wurden separate Bilder im VNIR- (400 nm – 1000 nm) und im SWIR-Bereich (1000 nm – 2500 nm) angefertigt. Das Blattreflexionsmodell PROSPECT-5b wurde auf zwei unterschiedliche Weisen invertiert: Durch numerische Inversion und durch einen Lookup-Table-Ansatz. Die Inversionsergebnisse aus dem VNIR-Datensatz alleine wurden mit denen aus dem kombinierten VNIR/SWIR-Datensatz verglichen. Es stellte sich heraus, dass die Inversionsmethode nur einen geringen Einfluss auf das Inversionsergebnis hat, wohingegen der Einfluss des Spektralbereichs für einige Variablen entscheidend ist. Während die Ergebnisse für den PROSPECT-Strukturparameter N, den Chlorophyllgehalt (Cab), den Carotenoidgehalt (Car) und die braunen Pigmente (Cbrown) für beide Eingangsdatensätze ähnlich sind, sind die Ergebnisse für den Wassergehalt (Cw) und die Trockenmasse (Cm) zwischen VNIR-Inversion und VNIR/SWIR-Inversion nicht korreliert. Es konnte gezeigt werden, dass laborbasierte abbildende Spektroskopie in Kombination mit der Inversion eines Strahlungstransfermodells in der Lage ist, chemische Blattparameter im Sub-Millimetermaßstab abzuleiten.

1 Introduction

Within-leaf variation of chemical and structural leaf properties has not gained much attention in the remote sensing community yet. In many reference measurements for remote sensing campaigns leaf properties are measured with devices like field spectrometers or chlorophyll metres (Asner et al. 2011, Buddenbaum et al. 2011). These typically measure certain spots on the leaf, but do not take the within-leaf variability into account. Laboratory imaging spectroscopy makes it pos-

www.schweizerbart.de
DOI: 10.1127/pfg/2015/0249
1432-8364/15/0249 $ 2.50

sible to investigate leaf properties on much smaller scales than traditional laboratory spectroscopy. Images with pixel sizes in the sub-millimetre range can be recorded in high spectral resolution (Steffens & Buddenbaum 2013). Each pixel contains a reflectance spectrum that can be used to derive chemical and structural leaf properties, either by statistical means or by reflectance model inversion (Schlerf & Atzberger 2006). The resulting leaf parameter maps can be used to assess the representability of spot measurements on the leaf or for studying biological processes in the leaf. In this study, we recorded hyperspectral images of two different leaves in the VNIR and in the SWIR spectral range, inverted the leaf reflectance model PROSPECT-5b for each pixel using two different inversion methods for VNIR and for full range datasets, respectively, and compared the results depending on spectral range and on the inversion method.

2 Material and Methods

2.1 *Hyperspectral Images*

Very high spatial resolution hyperspectral images of leaves were recorded using push-broom line scanners fixed in a laboratory frame. Usually, the scanners are installed in an airplane and the images are created by flying the airplane over the target. In the laboratory, a translation stage is placed under the scanners and moves the samples. The moving speed of the translation stage and the recording time of the scanners is adapted so that an image with square pixels results (Buddenbaum & Steffens 2011). The leaves were placed on a black rubber foam mat with very low and flat reflectance throughout the spectral region considered (Fig. 1). Images were recorded in the VNIR range using a HySpex VNIR-1600 camera (Stern et al. 2014) and in the SWIR range with a HySpex SWIR-320m-e camera (Norsk Elektro Optikk AS, Lørenskog, Norway, see Tab. 1 for sensor properties). VNIR images have a pixel size of about 62 µm × 62 µm, SWIR resolution is about 250 µm × 250 µm. An image-to-image geometric correction was applied to the SWIR image with the VNIR image as reference. The VNIR image was then resampled to SWIR spatial resolution and the images were joined. Furthermore, SWIR spectra were adapted multiplicatively to VNIR spectra: For the spectral overlap region of 970 nm to 990 nm the mean factor of brightness differences between both sensors was determined, and SWIR spectra were divided by this factor. A white reference panel with known reflectance was recorded with the leaves so that reflectance could be

Tab. 1: Properties of the hyperspectral scanners used.

	VNIR-1600	**SWIR-320m-e**
Detector	Si CCD, 1600 x 1200 pixel	HgCdTe, 320 x 256 pixel
Spectral range	410 nm – 990 nm	967 nm – 2500 nm
Spatial pixels	1600	320
FOV across track	16.75° (0.29 rad)	13.30° (0.23 rad)
IFOV across track / along track (instantaneous field of view, pixel)	0.01035° / 0.0207° (0.18 mrad / 0.36 mrad)	0.043° (0.75 mrad)
Spectral sampling	3.7 nm	6.0 nm
Number of bands	160	256
Digitization	12 bit	14 bit

calculated from recorded radiance (Peddle et al. 2001, Buddenbaum et al. 2012). The background was masked out of the image.

2.2 *Reflectance Model*

PROSPECT-5b (Féret et al. 2008, Jacquemoud & Baret 1990) is a plate model that simulates the directional-hemispherical reflectance and transmittance of a leaf from 400 nm to 2500 nm. The imaging spectrometers employed in this study measure the biconical reflectance factor (Schaepman-Strub et al. 2006). We assumed Lambertian behaviour (Fourty & Baret 1997) and neglected the difference between the two quantities here. In forward mode, structural and chemical leaf parameters are input to the model, and the model calculates leaf reflectance and transmittance spectra as output (Schlerf & Atzberger 2006). In an inversion, the spectra serve as input and the leaf parameters are output (Goel 1988). The inversion problem is not always solvable because there is always noise in the measurements, the model is never perfect, and different combinations of input parameters may lead to nearly identical spectra (ill-posed problem, Förster et al. 2010). Since in this study only reflectance has been measured, transmittance is not used.

While PROSPECT-3 and -4 only use the structure parameter (N), chlorophyll a+b content (Cab), water content (Cw), and dry matter content (Cm) as input parameters, PROSPECT-5 adds carotenoid content (Car), and PROSPECT-5b adds brown pigments content (Cbrown). The parameters are outlined in Tab. 2. Since the leaves considered contain brown patches we decided to use PROSPECT-5b in this study.

The reflective properties of leaves have been used to derive chemical leaf properties for a long time (Curran 1989). Since PROSPECT uses only a very limited amount of parameters, inversion is much easier than the inversion of canopy radiative transfer models (Jacquemoud et al. 2000, Koetz et al. 2004). We inverted the model in two different ways: by numerical inversion and by a lookup table (LUT) approach (Combal et al. 2002).

In a LUT inversion approach, a large number of spectra is modelled with known parameters in forward mode as a first step. In the inversion step, for a measured spectrum with unknown parameters the most similar modelled spectrum is searched among the LUT spectra and its parameters are used as inversion result. The LUT can be filled systematically, i.e., every parameter is varied in fixed steps and a spectrum is modelled with each combination of parameters, or randomly, i.e., a fixed number of spectra is modelled with random parameter values in a fixed range. Further possible variations include using different merit functions for determining the most similar spectrum (Féret et al. 2011) or using the mean or median of several most similar spectra (Koetz et al. 2004). For the LUT inversion in this study, 150,000 spectra were modelled with random values uniformly distributed in the range specified in Tab. 2 for the 6 input

Tab. 2: PROSPECT-5b parameters and boundaries for the inversion.

Parameter Name	Symbol	Unit	Minimum	Maximum
Structure parameter	N		0.8	3.0
Chlorophyll a+b content	Cab	µg/cm²	0	40
Carotenoids content	Car	µg/cm²	0	20
Brown pigments content	Cbrown	arbitrary units	0	4
Equivalent water thickness	Cw	g/cm² or cm	0.002	0.06
Dry matter content	Cm	g/cm²	0.001	0.02

variables of PROSPECT-5b (Darvishzadeh et al. 2011). The sum of squared differences between modeled and measured spectra for each wavelength was calculated as merit function for each pixel and the parameters of the nearest neighbour model spectrum were saved for each pixel.

Numerical inversions of reflectance models are less common in remote sensing. A mathematical optimisation routine is used to find the global minimum of deviation between modelled and measured spectra (Kuusk & Nilson 2000). Starting with an initial guess, parameters are varied within the given boundaries until a minimum is found. Some minimisation routines are discussed in Kimes et al. (2000). The numerical inversion was done in Matlab, using the function *fmincon* for constrained nonlinear multivariate function minimisation (Powell 1978, Mathworks 2014), similar to the approach by Jacquemoud (2011). Parameters of the numeric inversion were also constrained to the values specified in Tab. 2.

Since no hard reference data of leaf properties in the high resolution necessary is available we only report correlations of the different inversion results. When a parameter is estimated consistently independent of the inversion method or the input data we assume that the inversions results for this parameter are close to the "true" value, while inconsistent inversion results, i.e. low correlations, hint to unreliable estimations of this parameter in at least one of the considered cases. Additionally, when the parameter is mapped for the whole leaf and the image has low noise and shows leaf structures well, the inversion of this parameter is considered consistent and thus more reliable than a parameter that leads to a noisy map.

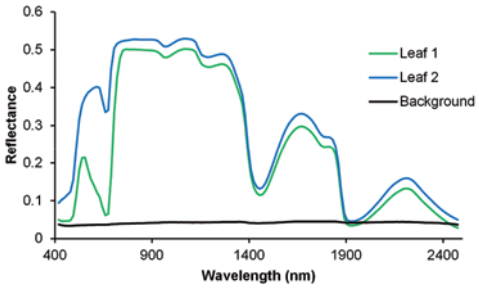

Fig. 1: Mean spectra of the two leaves and the background.

3 Results

3.1 *Hyperspectral Images*

Mean spectra of the two leaves are shown in Fig. 1. It can be clearly seen that leaf 1 is a healthy green leaf while leaf 2 is brownish-yellowish and not very healthy. Fig. 2 depicts a true-colour and a false-colour representation of the leaves. One leaf is medium green and healthy, the other one is yellowish-brown with chlorosis patches. Four spectra are displayed. The left part of the figure only shows the VNIR spectra, in the right part VNIR and SWIR spectra are combined. The top left spectrum is a typical leaf spectrum showing the well-known features of absorption in the blue and red wavelength regions, green peak, red edge, near-infrared plateau and water absorption bands at 970 nm, 1200 nm, 1450 nm, and 1950 nm. The bottom left spectrum shows the reflectance of a leaf vein with less pronounced

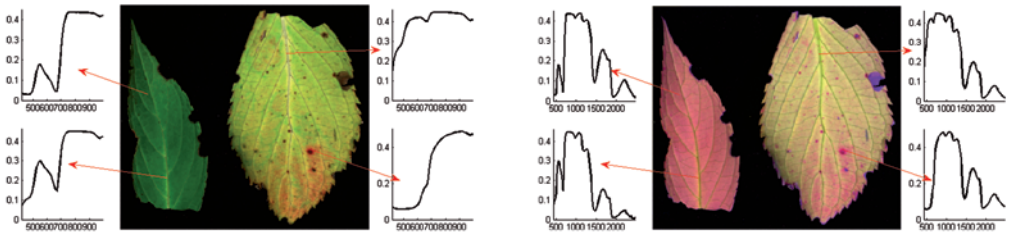

Fig. 2: Left: True colour image (RGB: 645 nm, 555 nm, 450 nm) and exemplary VNIR spectra of the two leaves considered, right: false-colour image (RGB: 795 nm, 555 nm, 1575 nm) and exemplary VNIR/SWIR spectra.

chlorophyll absorption and more pronounced water absorption. The right spectra do not have a green peak. The top right spectrum is of a yellow area next to the leaf vein, the bottom right spectrum shows the reflectance of a brown patch.

3.2 *Inversion Results*

Inversion results using only VNIR images and combined VNIR/SWIR (full range) images are compared in the following figures.

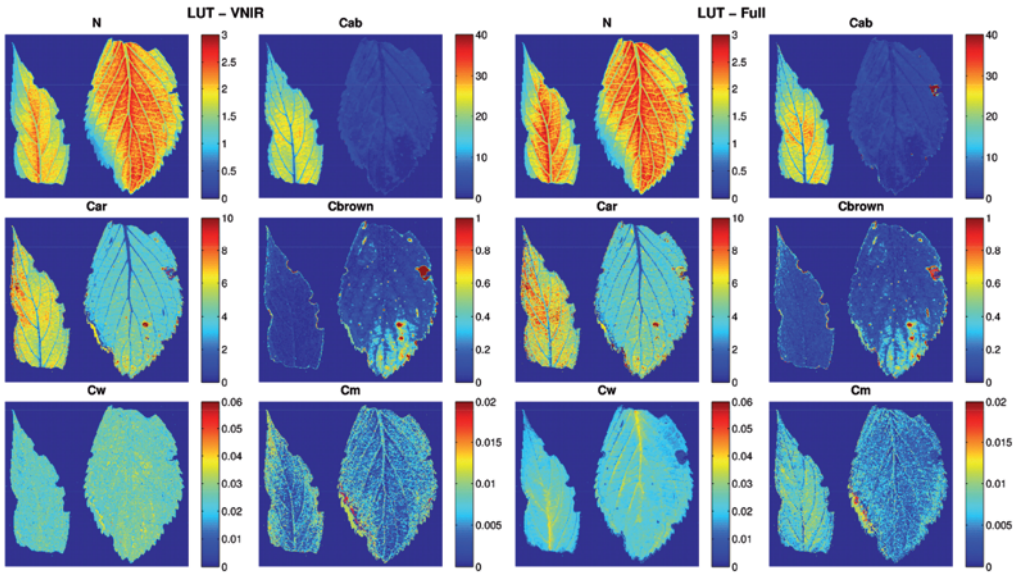

Fig. 3: Maps of PROSPECT-5b parameters resulting from lookup table inversion (LUT). Left: VNIR input data, right: full range input data.

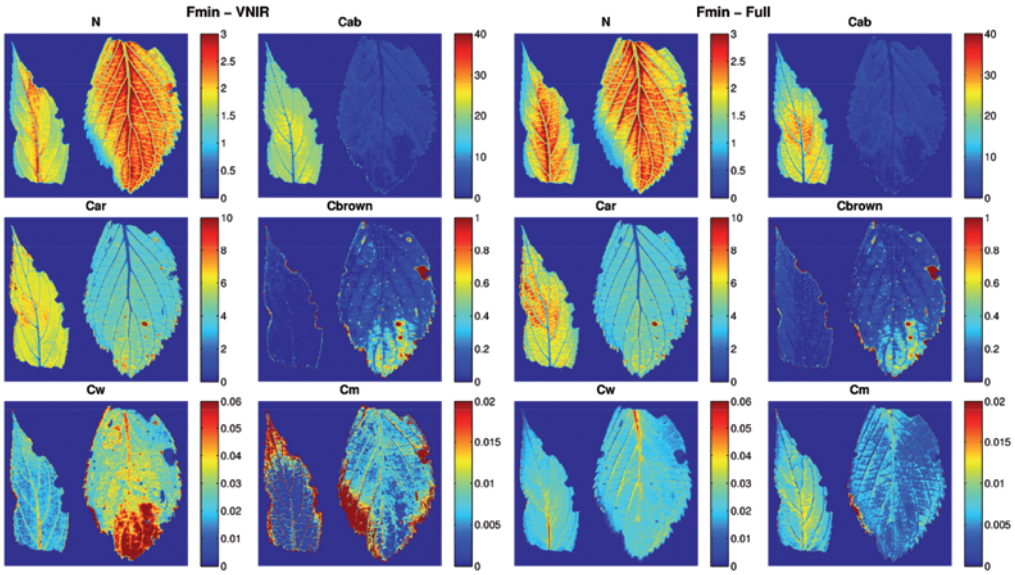

Fig. 4: Maps of PROSPECT-5b parameters resulting from numeric minimisation inversion (fmin). Left: VNIR only, right: VNIR/SWIR.

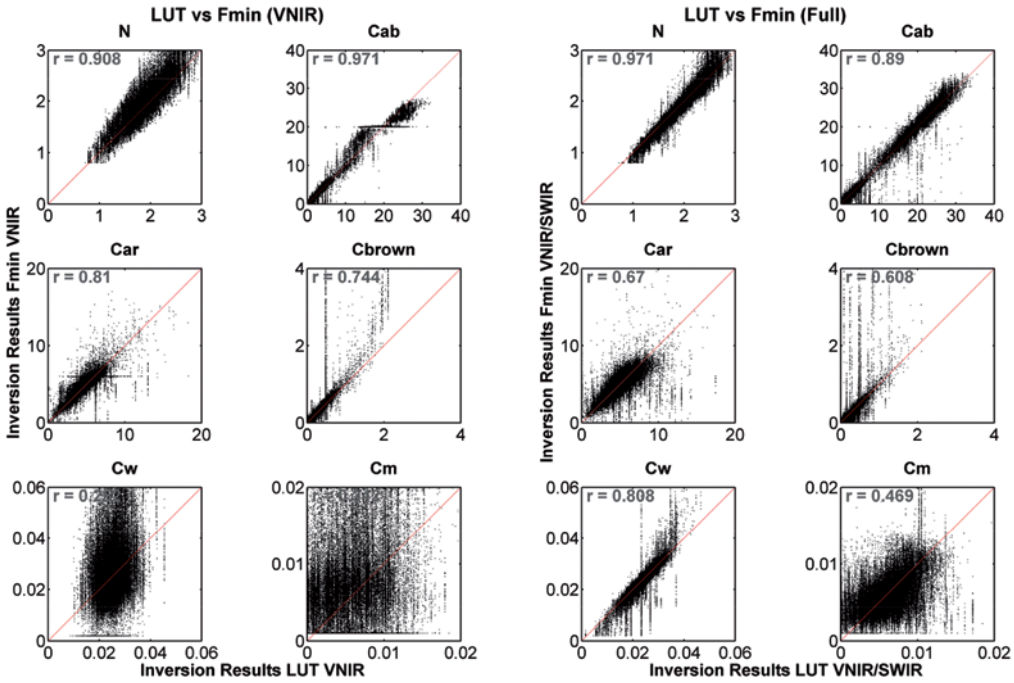

Fig. 5: Comparison of inverted PROSPECT-5b parameters, LUT inversion against numeric minimisation (Fmin). Left: VNIR only, right: VNIR/SWIR.

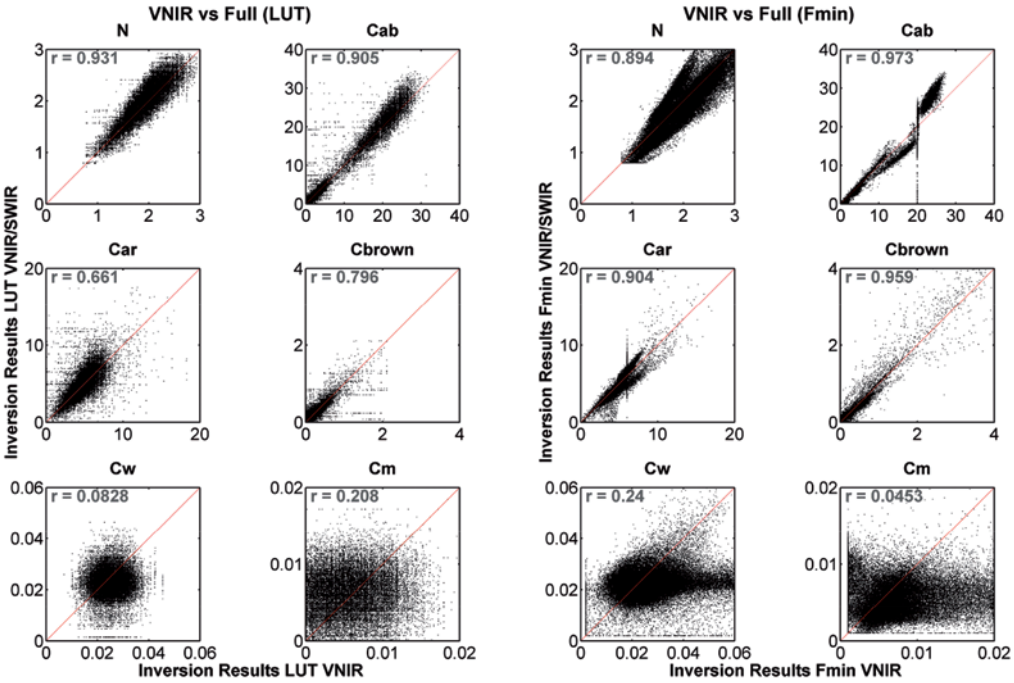

Fig. 6: Comparison of PROSPECT-5b parameter inversions, VNIR against VNIR/SWIR. Left: Lookup table, right: numeric inversion.

Figs. 3 and 4 show resulting maps of PROSPECT-5b parameters from the different inversions. In Fig. 3 the LUT inversions are depicted, with VNIR input data on the left, and full range input data on the right. Fig. 4 shows the respective numeric minimisation inversions. Some structures within the leaves are clearly discernible. E.g., the carotenoid (Car) values in the veins are very low, while the full range images show that the water content (Cw) is highest in the veins. The VNIR images of water content, on the other hand, do not show clear structures and are very noisy. The brown spots on the right leaf are clearly shown by all inversion results of Cbrown. All maps of dry matter content (Cm) are noisy and differences between the methods are large. The largest difference between the two leaves is in the chlorophyll content (Cab) which is much higher in the left leaf than in the right. The correlations of the corresponding pixels between pairs of images of the same parameter for these four inversions are depicted in Figs. 5 and 6. Fig. 5 compares the inversion techniques, i.e. LUT against numeric minimisation inversion, for VNIR and for VNIR/SWIR input data. Fig. 6 compares input datasets for both inversion techniques. The correlations of the inverted PROSPECT parameters have values between 0.04 and 0.97.

The images were inverted on a pixel-by-pixel basis, and additionally the mean leaf spectra shown in Fig. 1 were inverted. Fig. 7 displays histograms of the resulting PROSPECT-5b parameters for the two leaves, i.e., numeric minimisation using VNIR/SWIR full range spectra, to show the intra-leaf variability, and inverted parameters for the mean spectra of the two leaves as red lines. For most parameters, the result for the mean leaf spectrum is close to the modal value of the single pixel inversions, but there is always a considerable variance. The largest deviation between the modal value and the inverted value for the mean leaf spectrum is at the structure parameter N of leaf 2.

4 Discussion

The results were mostly in accordance with the expectations. The inversion of PROSPECT usually leads to reasonable results (LE MAIRE et al. 2004), so image-based inversion led to reasonable parameter maps partially depending on the spectral range used. It could

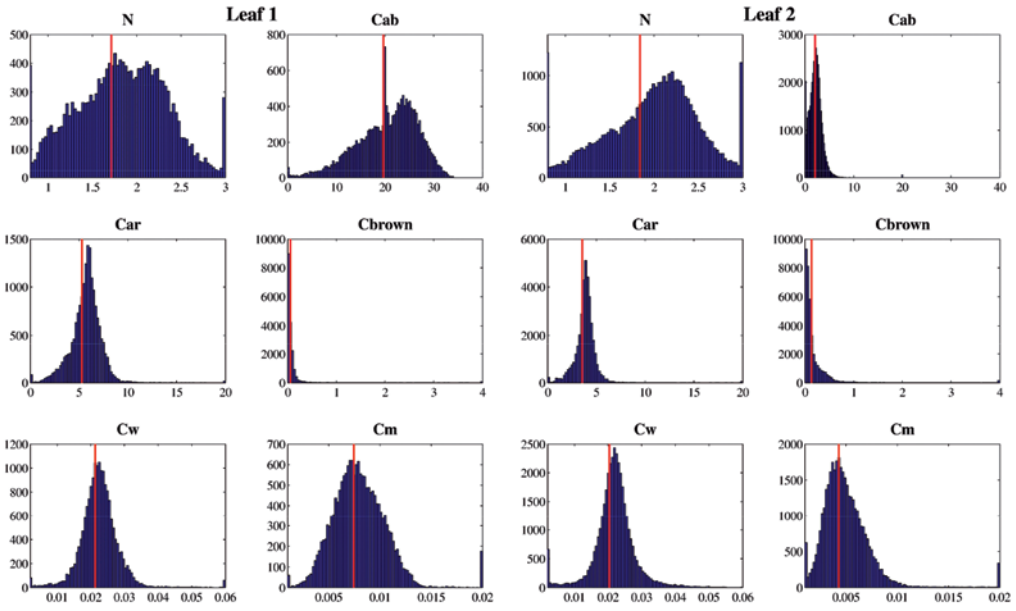

Fig. 7: Intra-leaf variation: Histograms of inverted PROSPECT parameters and inverted values for mean leaf spectrum as shown in Fig. 1 (red line) for the two leaves.

be shown that the inversion also works with laboratory hyperspectral images so that leaf parameters can be mapped in sub-millimetre resolution.

We found that the inversion technique has only minor influence on inversion results, but the spectral range of the input data is crucial for some variables: While results for the PROSPECT structure parameter N, chlorophyll content (Cab), carotenoid content (Car) and brown pigments (Cbrown) are similar for both input datasets, results for water content (Cw) and dry matter (Cm) are not correlated between VNIR inversion and full range inversion. Since the first four parameters are optically active in the VNIR range, the coherent results are unsurprising (Sims & Gamon 2002). The finding that the inversion accuracy for Cm is lower than for other parameters is in accordance with other studies (e.g. Atzberger & Richter 2012, Stuckens et al. 2009, Féret et al. 2008, Riaño et al. 2005).

For some pixels, the Fmin inversion of Cab is stuck at the initial value of 20. An analysis of the affected pixels showed that these are dark pixels at the edge of the leaf which generally are the areas with highest deviation between modelled and measured spectra. In these pixels, the algorithm stops after the maximum value of 5,000 iterations without a satisfactory solution. A buffering of leaf edges could resolve this problem.

Key findings of this study are:

- Laboratory-based imaging spectroscopy is an appropriate technique for very-high resolution mapping of reflectance.
- Laboratory-based imaging spectroscopy combined with inversion of the PROSPECT leaf reflectance model is well suited for mapping chemical and structural leaf properties.
- Results for PROSPECT structure parameter N are consistent regardless of inversion method and spectral range.
- Chlorophyll a+b content (Cab) results are also highly correlated. Fmin inversion sometimes favours certain values, e.g. Cab = 20. Since Cab absorbs in the visible domain, SWIR information is not necessary.
- The same holds for the PROSPECT-5b specific variables Carotenoid content (Car) and Brown Leaf Matter (Cbrown): Their main absorption features are in the visible and near infrared range, so SWIR is not needed. In the VNIR/SWIR LUT inversion of Car, the SWIR even seems to introduce some image noise.
- The leaf water content (Cw) can only be estimated well with SWIR information. There is no correlation between the two spectral ranges. Correlation between the two techniques using full range spectra is very high.
- Dry matter content (Cm) estimations are the least reliable with low correlations for all comparisons.

5 Conclusions

Intra-leaf variability of leaf optical properties can be measured using laboratory imaging spectroscopy. We were able to invert the leaf reflectance model PROSPECT-5b to infer leaf constituents and structure on a sub-millimetre scale. Measurements like this can be used to evaluate reference measurements on the leaf level or simply to study leaves and the spatial distribution of leaf constituents. While N and Cab inversions are relatively straightforward and independent of inversion technique and input dataset, Cw and Cm inversions are more difficult so that there is much more scatter und less correlation between the different inversions. Car and Cbrown are parameters with intermediate correlation between the different inversions.

Acknowledgements

This work was supported within the framework of the EnMAP project (contract No. 50EE1258) by the German Aerospace Center (DLR) and the Federal Ministry of Economics and Technology. The authors would like to thank three anonymous reviewers for the helpful comments.

References

Asner, G.P., Martin, R.E., Knapp, D.E., Tupayachi, R., Anderson, C., Carranza, L., Martinez, P., Houcheime, M., Sinca, F. & Weiss, P., 2011:

Spectroscopy of canopy chemicals in humid tropical forests. – Remote Sensing of Environment **115:** 3587–3598.

Atzberger, C. & Richter, K., 2012: Spatially constrained inversion of radiative transfer models for improved LAI mapping from future Sentinel-2 imagery. – Remote Sensing of Environment **120:** 208–218.

Buddenbaum, H., Pueschel, P., Stellmes, M., Werner, W. & Hill, J., 2011: Measuring water and Chlorophyll content on the leaf and canopy scale. – EARSeL eProceedings **10:** 66–72.

Buddenbaum, H. & Steffens, M., 2011: Laboratory imaging spectroscopy of soil profiles. – Journal of Spectral Imaging **2:** 1–5.

Buddenbaum, H., Stern, O., Stellmes, M., Stoffels, J., Pueschel, P., Hill, J. & Werner, W., 2012: Field Imaging Spectroscopy of Beech Seedlings under Dryness Stress. – Remote Sensing **4** (12): 3721–3740.

Combal, B., Baret, F., Weiss, M., Trubuil, A., Macé, D., Pragnère, A., Myneni, R., Knyazikhin, Y. & Wang, L., 2002: Retrieval of canopy biophysical variables from bidirectional reflectance using prior information to solve the ill-posed inverse problem. – Remote Sensing of Environment **84:** 1–15.

Curran, P.J., 1989: Remote sensing of foliar chemistry. – Remote Sensing of Environment **30** (3): 271–278.

Darvishzadeh, R., Atzberger, C., Skidmore, A. & Schlerf, M., 2011: Mapping grassland leaf area index with airborne hyperspectral imagery: A comparison study of statistical approaches and inversion of radiative transfer models. – ISPRS Journal of Photogrammetry and Remote Sensing **66** (6): 894–906.

Féret, J.-B., François, C., Asner, G.P., Gitelson, A.A., Martin, R.E., Bidel, L.P.R., Ustin, S.L., le Maire, G. & Jacquemoud, S., 2008: PROSPECT-4 and 5: Advances in the leaf optical properties model separating photosynthetic pigments. – Remote Sensing of Environment **112:** 3030–3043.

Féret, J.-B., François, C., Gitelson, A., Asner, G.P., Barry, K.M., Panigada, C., Richardson, A.D. & Jacquemoud, S., 2011: Optimizing spectral indices and chemometric analysis of leaf chemical properties using radiative transfer modeling. – Remote Sensing of Environment **115:** 2742–2750.

Förster, M., Spengler, D., Buddenbaum, H., Hill, J. & Kleinschmit, B., 2010: Ein Überblick über die Kombination spektraler und geometrischer Modellierung zur Anwendung in der forstlichen Fernerkundung. – PFG – Photogrammetrie, Fernerkundung, Geoinformation **2010** (4): 253–265.

Fourty, T. & Baret, F., 1997: Vegetation water and dry matter contents estimated from top-of-the-atmosphere reflectance data: A simulation study. – Remote Sensing of Environment **61** (1): 34–45.

Goel, N.S., 1988: Models of vegetation canopy reflectance and their use in estimation of biophysical parameters from reflectance data. – Remote Sensing Reviews **4** (1): 1–212.

Jacquemoud, S., Bacour, C., Poilvé, H. & Frangi, J.-P., 2000: Comparison of four radiative transfer models to simulate plant canopies reflectance: direct and inverse mode. – Remote Sensing of Environment **74:** 471–481.

Jacquemoud, S., 2011: Prospect + Sail = Prosail. – http://teledetection.ipgp.jussieu.fr/prosail/ (26.1.2015).

Jacquemoud, S. & Baret, F., 1990: PROSPECT: a model of leaf optical properties spectra. – Remote Sensing of Environment **34:** 75–91.

Kimes, D.S., Knyazikhin, Y., Privette, J.L., Abuelgasim, A.A. & Gao, F., 2000: Inversion methods for physically-based models. – Remote Sensing Reviews **18** (2–4): 381–439.

Koetz, B., Schaepman, M., Morsdorf, F., Bowyer, P., Itten, K. & Allgöwer, B., 2004: Radiative transfer modeling within a heterogeneous canopy for estimation of forest fire fuel properties. – Remote Sensing of Environment **92:** 332–344.

Kuusk, A. & Nilson, T., 2000: A Directional Multispectral Forest Reflectance Model. – Remote Sensing of Environment **72** (2): 244–252.

le Maire, G., François, C. & Dufrêne, E., 2004: Towards universal broad leaf chlorophyll indices using PROSPECT simulated database and hyperspectral reflectance measurements. – Remote Sensing of Environment **89** (1): 1–28.

Mathworks, 2014: fmincon. – http://www.mathworks.de/de/help/optim/ug/fmincon.html (7.10.2014).

Peddle, D.R., White, H.P., Sofer, R.J., Miller, J.R. & LeDrew, E.F., 2001: Reflectance processing of remote sensing spectroradiometer data. – Computers & Geosciences **27:** 203–213.

Powell, M.J.D., 1978: A Fast Algorithm for Nonlinearly Constrained Optimization Calculations. – Watson, G.A. (ed.): Lecture Notes in Mathematics **630**, Springer-Verlag.

Riaño, D., Vaughan, P., Chuvieco, E., Zarco-Tejada, P.J. & Ustin, S.L., 2005: Estimation of fuel moisture content by inversion of radiative transfer models to simulate equivalent water thickness and dry matter content: analysis at leaf and canopy level. – IEEE Transactions on Geoscience and Remote Sensing **43** (4): 819–826.

Schaepman-Strub, G., Schaepman, M.E., Painter, T.H., Dangel, S. & Martonchik, J.V., 2006: Reflectance quantities in optical remote sensing – definitions and case studies. – Remote Sensing of Environment **103** (1): 27–42.

Schlerf, M. & Atzberger, C., 2006: Inversion of a forest reflectance model to estimate structural canopy variables from hyperspectral remote sensing data. – Remote Sensing of Environment **100:** 281–294.

Sims, D.A. & Gamon, J.A., 2002: Relationships between leaf pigment content and spectral reflectance across a wide range of species, leaf structures and developmental stages. – Remote Sensing of Environment **81** (2–3): 337–354.

Steffens, M. & Buddenbaum, H., 2013: Laboratory imaging spectroscopy of a stagnic luvisol profile – High resolution soil characterisation, classification and mapping of elemental concentrations. – Geoderma **195-196:** 122–132.

Stern, O., Paschmionka, B., Stoffels, J., Buddenbaum, H. & Hill, J., 2014: Abbildende und nichtabbildende Geländespektrometrie zur Untersuchung von Stressphänomenen an Buchenpflanzen. – PFG – Photogrammetrie, Fernerkundung, Geoinformation **2014** (1): 17–26.

Stuckens, J., Verstraeten, W.W., Delalieux, S., Swennen, R. & Coppin, P., 2009: A dorsiventral leaf radiative transfer model: Development, validation and improved model inversion techniques. – Remote Sensing of Environment **113** (12): 2560–2573.

Address of the Authors:

Dr. Henning Buddenbaum & Prof. Dr. Joachim Hill, Universität Trier, Environmental Remote Sensing & Geoinformatics, D-54286 Trier, Germany, Tel.: +49-651-201-4729, e-mail: {buddenbaum}{hillj}@uni-trier.de

Manuskript eingereicht: Juli 2014
Angenommen: Januar 2015